

Push–Pull Quinonoid Compounds: Enhanced Powder SHG Utilizing the Effect of Chiral Centers on the Dipole Alignment

M. Ravi,[†] D. Narayana Rao,[‡] Shmuel Cohen,[§] Israel Agranat,[⊥] and T. P. Radhakrishnan^{*,†}

School of Chemistry and School of Physics, University of Hyderabad, Hyderabad 500 046, India, and Department of Inorganic Chemistry and Department of Organic Chemistry, The Hebrew University of Jerusalem, Jerusalem 91904, Israel

Received October 9, 1996. Revised Manuscript Received January 7, 1997[Ⓡ]

The molecular and crystal structure of a chiral diamino-substituted dicyanoquinodimethane and the observation of strong solid-state optical second harmonic generation (SHG) in this material are reported. The enhanced SHG was obtained by exploiting the strong influence of the rigidity of the stereogenic center environment on the alignment of the molecular dipole vectors. The intervector angles in this class of materials are found to correlate well with the powder SHG. Since a strong molecular twist (of the diaminomethylene unit with respect to the quinonoid ring) of $\sim 50^\circ$ is found in this class of compounds, the dependence of the molecular hyperpolarizability (β) on the twist was examined. The interesting observation was that the computed β attained the maximum value at the twist angle corresponding to the optimized molecular structure, which in turn closely resembled the structure obtained from single-crystal X-ray analysis. This unusual behavior of β is explained on the basis of the two-state model.

Introduction

Currently there is a great deal of interest in developing molecular and polymeric materials for nonlinear optical applications, touted as the basis for future photonic technologies.^{1–8} Several donor–acceptor substituted π -electron conjugated organic molecules with their fast and efficient quadratic nonlinear optical (NLO) responses are promising candidates for applications such as second harmonic generation (SHG). The crucial steps involved in the development of molecular materials for SHG are (i) the synthesis of molecules with large hyperpolarizabilities, β , and (ii) the assembly of these molecules into a suitable noncentric lattice so that the molecular nonlinear responses add up to a strong bulk response. Though β is best assessed by experimental methods such as electric field induced second harmonic generation (EFISHG) or hyper Rayleigh scattering (HRS), a fairly reliable estimate can be obtained using quantum chemical computations. The β can often be fine-tuned by tailoring the molecular skeleton or the

electron-donating and -accepting groups. The fabrication of the noncentric assembly of molecules is a more difficult problem due to the tendency of many organic molecules, especially those with strong ground-state dipole moments, to pack in centrosymmetric crystal lattices. Methods such as electric field poling,^{9–10} oriented film growth through Langmuir–Blodgett techniques,^{11,12} salt formation,^{13,14} and the use of optically active modifications^{4,15,16} are used to fabricate a noncentric arrangement of the NLO chromophores.

Recently we have embarked upon a systematic investigation of a class of push–pull quinonoid molecules (Figure 1) as novel molecular materials for quadratic NLO applications. These compounds are based on diamino-substituted dicyanoquinodimethanes first synthesized by a du Pont group^{17a} in 1962 and investigated very briefly by some earlier workers.^{17b–d} Our semiempirical quantum chemical studies¹⁸ showed that they

(9) Burland, D. M.; Miller, R. D.; Walsh, C. A. *Chem. Rev. (Washington, D.C.)* **1994**, *94*, 31.

(10) Choi, D. H.; Wijekoon, W. M. K. P.; Kim, H. M.; Prasad, P. N. *Chem. Mater.* **1994**, *6*, 234.

(11) Ashwell, G. J.; Dawnay, E. J. C.; Kuczynski, A. P.; Szablewski, M.; Sandy, I. M. *J. Chem. Soc., Faraday Trans.* **1990**, *86*, 1117.

(12) Ashwell, G. J.; Jefferies, G.; Hamilton, D. G.; Lynch, D. E.; Roberts, M. P. S.; Bahra, G. S.; Brown, C. R. *Nature* **1995**, *375*, 385.

(13) Marder, S. R.; Perry, J. W.; Schaefer, W. P. *Science* **1989**, *245*, 626.

(14) Marder, S. R.; Perry, J. W.; Yakymyshyn, C. P. *Chem. Mater.* **1994**, *6*, 1137.

(15) Zyss, J.; Nicoud, J. F.; Coquillay, M. *J. Chem. Phys.* **1984**, *81*, 4160.

(16) Ukachi, T.; Shigemoto, T.; Komatsu, H.; Sugiyama, T. *J. Opt. Soc. Am. B* **1993**, *10*, 1372.

(17) (a) Hertler, L. R.; Hartzler, H. D.; Acker, D. S.; Benson, R. E. *J. Am. Chem. Soc.* **1962**, *84*, 3387. (b) Nicoud, J.-F.; Twieg, R. J. In *Nonlinear Optical Properties of Organic Molecules and Crystals*; Chemla, D. S., Zyss, J., Eds.; Academic Press: New York, 1987; Vol. 1, p 227. (c) Chemla, D. S., Zyss, J., Eds.; *Nonlinear Optical Properties of Organic Molecules and Crystals*; Academic Press: New York, 1987; Vol. 2, p 221. (d) Nicoud, J. F. *Mol. Cryst. Liq. Cryst.* **1988**, *156*, 257.

[†] School of Chemistry.

[‡] School of Physics.

[§] Department of Inorganic Chemistry.

[⊥] Department of Organic Chemistry.

[Ⓡ] Abstract published in *Advance ACS Abstracts*, February 15, 1997.

(1) Williams, D. J. *Nonlinear Optical Properties of Organic and Polymeric Materials*; ACS Symp. Ser. 233; American Chemical Society: Washington, DC, 1983.

(2) Williams, D. J. *Angew. Chem., Int. Ed. Engl.* **1984**, *23*, 690.

(3) Chemla, D. S., Zyss, J., Eds. *Nonlinear Optical Properties of Organic Molecules and Crystals*; Academic Press: New York, 1987.

(4) Eaton, D. F. *Science* **1991**, *253*, 281.

(5) Prasad, P. N.; Williams D. J. *Introduction to Nonlinear Optical Effects in Organic Molecules and Polymers*; Wiley: New York, 1991.

(6) Nie, W. *Adv. Mater.* **1993**, *5*, 520.

(7) Kanis, D. R.; Ratner, M. A.; Marks, T. J. *Chem. Rev. (Washington, D.C.)* **1994**, *94*, 195.

(8) Marks, T. J.; Ratner, M. A. *Angew. Chem., Int. Ed. Engl.* **1995**, *34*, 155.

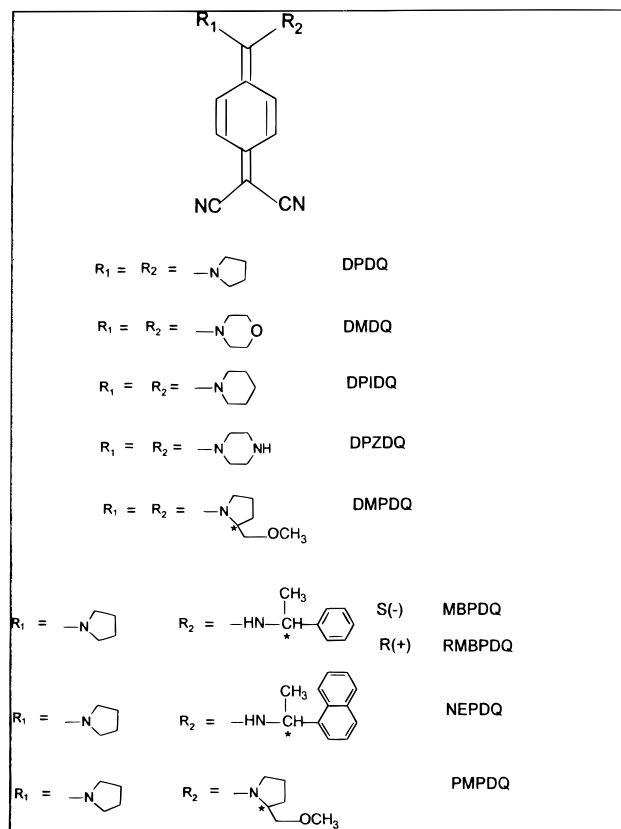


Figure 1. Molecular structure of di-amino-substituted dicyanoquinodimethanes; the abbreviations of the names are discussed in the text.

have appreciable β values, in agreement with the EFISHG study of the prototypical system, 2-(4-(dicyanomethylene)cyclohexa-2,5-dienylidene)imidazolidine.¹⁹ Theoretical studies also showed that the β could be fine-tuned by controlling the electron-donating and -accepting capability of the push–pull groups.²⁰ Preliminary experimental studies indicated that these materials possessed the following positive features: (i) easy synthesis and flexibility to introduce a variety of substituent groups, (ii) good crystal growth of several derivatives, (iii) thermal stability up to 250–300 °C, and (iv) optical transparency through most of the visible region, with absorption maxima typically around 350–400 nm.^{18,21,22} The main drawback appears to be the large ground-state dipole moment which often leads to the formation of centrosymmetric crystal lattices.²¹ We were able to obtain noncentrosymmetric crystals by introducing chiral groups at the donor end of these systems, and these materials showed moderate-to-strong SHG capability; powder studies showed them to be phase-matchable materials.²²

A careful analysis of the crystal structures of the two chiral systems studied earlier,²² 7-*S*(–)-(α-methylbenzylamino)-7-pyrrolidino-8,8-dicyanoquinodimethane (MBPDQ) and 7-*S*(+)-2-(methoxymethyl)pyrrolidino-7-pyr-

rolidino-8,8-dicyanoquinodimethane (PMPDQ, Figure 1), revealed that even though the introduction of chirality led to crystallographic noncentrosymmetry in both cases, the molecular dipole moment vectors (approximated as the vector from the diaminomethylene carbon to the dicyanomethylene carbon) were still fairly close to an antiparallel arrangement. Therefore it was clear that we were not realizing yet the full potential of these molecular materials in terms of their SHG efficiency. In MBPDQ, the stereogenic center is on a conformationally flexible side group, and in PMPDQ, it is on a relatively more rigid cyclic moiety. This feature has led to larger deviation of dipole vectors from an antiparallel orientation, and consequently an improvement in the SHG capability from MBPDQ (3 U) to PMPDQ (28 U) (1 U = SHG efficiency of urea). Thus it appeared that the introduction of two stereogenic centers of the more rigid type close to the dipole axis would lead to still higher SHG capability. We report in this paper the synthesis and characterization of 7,7-di(*S*(+)-2-(methoxymethyl)pyrrolidino)-8,8-dicyanoquinodimethane (DMPDQ, Figure 1), its molecular and crystal structure, and the dramatic improvement of the SHG capability to ~55 U in this material.

In all the molecular structures we have investigated in this class of diamino-substituted dicyanoquinodimethanes, the diaminomethylene group is strongly twisted out of the plane containing the quinonoid ring and the dicyanomethylene unit. In a comparative study of the molecular structures obtained from crystal structure analysis and AM1 semiempirical optimization, we noticed that the molecular hyperpolarizabilities showed some correlation to this molecular twist. This prompted us to probe more systematically the dependence of β on the molecular twist, and we report in this paper the results of these studies on the model system, 7,7-dipyrrolidino-8,8-dicyanoquinodimethane (DPDQ, Figure 1). The surprising observation is that the β as a function of the twist angle reaches a maximum at the fully optimized geometry from AM1 computation, which in turn has a close correspondence to the molecular structure obtained from the crystal analysis. On the basis of the well-known two-state model,²³ we discuss the factors that lead to the maximization of β at the optimal geometry.

Experimental Section

DMPDQ was synthesized following the procedure reported for similar compounds in ref 17a. Tetracyanoquinodimethane (TCNQ, 0.10 g, 0.49 mmol) was dissolved in 20 mL of tetrahydrofuran (freshly distilled and dried over sodium). To this solution, 0.18 mL (1.46 mmol) of *S*(+)-2-(methoxymethyl)pyrrolidine was added. The solution turned dark green immediately and changed to greenish yellow on heating at 50 °C and stirring for ~2 min. A greenish yellow precipitate appeared slowly. The solution was then cooled to 30 °C and kept for 2 h. After further cooling to 5 °C for half an hour, the precipitate was filtered out and washed with cold tetrahydrofuran to give 60% yield of a greenish yellow compound. Recrystallization from acetonitrile gave pale yellow, transparent, prismlike crystals, melting point 250 °C; FTIR (KBr pellet) 2172, 2133 (conjugated nitrile stretch), 1590 and 1450 (CH₂–O–CH₃ stretch) cm^{–1}; UV–vis (acetonitrile solution) 406 nm; MS(EI) *m/z* = 380 (85), 83(6), 70(22), 69(22), 45(23), 40(100). Elemental analysis (calculated for C₂₂N₄O₂H₂₈): C, 70.06

(18) Ravi, M.; Narayana Rao, D.; Cohen, S.; Agranat, I.; Radhakrishnan, T. P. *Curr. Sci. (India)* **1995**, *68*, 1119.

(19) Lalama, S. J.; Singer, K. D.; Garito, A. F.; Desai, K. N. *Appl. Phys. Lett.* **1981**, *39*, 940.

(20) Ravi, M.; Radhakrishnan, T. P. *J. Phys. Chem.* **1995**, *99*, 17624.

(21) Ravi, M.; Cohen, S.; Agranat, I.; Radhakrishnan, T. P. *Struct. Chem.* **1996**, *7*, 225.

(22) Ravi, M.; Narayana Rao, D.; Cohen, S.; Agranat, I.; Radhakrishnan, T. P. *J. Mater. Chem.* **1996**, *6*, 1119.

(23) Oudar, J. L. *J. Chem. Phys.* **1977**, *67*, 446.

(69.47); H, 7.83 (7.37); N, 14.43 (14.74). Optical rotation, $\alpha_{25}^D = +485^\circ$ ($c = 0.04$, methanol).

Crystal structure data was collected on an Enraf-Nonius CAD4 computer-controlled diffractometer. Cu K α ($\lambda = 1.54178$ Å) radiation with a graphite crystal monochromator in the incident beam was used. The standard CAD4 centering, indexing, and data collection software were used. The unit-cell dimensions were obtained by a least-squares fit of 24 centered reflections in the range $24 \leq \theta \leq 30^\circ$. Other details of data collection and refinement, thermal parameters, bond lengths, angles, least-squares planes, and structure factors are available in the Supporting Information.

Powder SHG measurements were carried out using the Kurtz-Perry technique²⁴ with the fundamental wavelength (1064 nm) of a Q-switched Nd:YAG laser. The powders were graded on the basis of the particle sizes using standard sieves and packed between glass plates. The sample thickness was maintained constant by means of uniform 0.2 mm thick Teflon sheets inserted as spacers between the glass plates. The SHG intensity was calibrated using powder samples of urea with particle size ~ 150 μm . Samples showed no sign of decomposition even on prolonged irradiation with a laser power of 1 GW cm^{-2} (6 ns, 10 Hz).

Theoretical Methods

The computations reported in this paper were carried out using the MOPAC93 program.²⁵ Molecular structure optimizations were carried out using the AM1 method²⁶ with the PRECISE keyword; full geometry relaxation was usually allowed, and constraints imposed, if any, are discussed at the appropriate places. For calculations involving the excited state (for excitation energy, transition dipole, dipole moment changes, etc.) the corresponding ground-state optimized geometry was used and a configuration interaction (CI) scheme involving all single and pair excitations within a manifold of 10 molecular orbitals (five HOMOs and five LUMOs) was employed, invoking the keyword MICROS and reading in the 76 microstates.

Molecular hyperpolarizabilities, β were calculated using the time-dependent Hartree-Fock (TDHF) method^{27a} implemented in MOPAC93. The computed values are in very good agreement with the values obtained from MOPAC 6.0, which employs the finite field (FF) method.^{27b} The value of the static hyperpolarizabilities, $\beta(0)$, we report in this paper are the magnitude of the average β vector, scaled by a factor of 0.5 to make it comparable to experimental data. We note that the hyperpolarizabilities of the molecules we study are all negative. This arises from the decrease in dipole moment on excitation of these zwitterionic molecules, which we have verified experimentally by the observation of negative solvatochromism.

Results and Discussion

Facile substitution of two cyano groups in TCNQ by primary or secondary amines leading to the formation of diamino-substituted dicyanoquinodimethanes, first reported^{17a} in 1962, is a simple and versatile synthetic protocol; the synthesis conditions are very moderate and the purification procedures routine. We have exploited

this reaction to synthesize a number of push-pull quinonoid systems.^{18,21,22} The compounds were purified by simple recrystallization from solution, and many derivatives crystallized well. They are thermally quite stable, usually melting at 250–300 °C. The crystals are light yellow and nearly transparent, and show an absorption maximum in solution near 400 nm. Semiempirical computations revealed that, considering their sizes, these molecules have appreciably high β with the static values ($\beta(0)$) typically in the range -30 to -50×10^{-30} esu.

Several early candidates such as DPDQ and the dimorpholino, dipiperidino, and dipiperazino derivatives (DMDQ, DPIDQ, and DPZDQ in Figure 1) that we synthesized formed centrosymmetric crystals,²¹ presumably due to the strong ground-state dipole moments of these zwitterionic molecules. Our attempts to pole these molecules embedded in polymer films and silica gels were not successful. Introduction of chiral groups to introduce noncentrosymmetry in the crystal lattice was the next approach we adopted. On the basis of the early work on these push-pull quinonoids, we prepared the monopyrrolidine derivative of TCNQ, 7-pyrrolidino-7,8,8-tricyanoquinodimethane, so that the remaining cyano group at C7 can be substituted by a variety of chiral groups. Introduction of *S*(-)-methylbenzylamine led to the first compound MBPDQ in this series which crystallized in a noncentric space group ($P2_1$; $a = 12.715(3)$ Å, $b = 8.068(2)$ Å, $c = 10.422(2)$ Å; $\beta = 91.03(2)^\circ$; $z = 2$) and showed a solid-state SHG capability of ~ 3 U.¹⁸ Investigation of the SHG as a function of particle size indicated that the SHG was phase-matchable. The crystal structure of MBPDQ²² indicated that, though noncentrosymmetry was achieved, the molecular dipole vectors of adjacent NLO chromophores were nearly antiparallel. The low SHG capability of the material could be attributed to this. The *R*(+)-methylbenzylamine and the *S*(+)-naphthylethylamine derivatives (RMBPDQ and NEPDQ in Figure 1) did not show any improved SHG.²² The stereogenic centers in these molecules are on a side chain, and the center of symmetry is broken by small bond rotations rather than reorientation of the molecular dipoles. The stereogenic center in a more rigid environment would force the near-neighbor molecular dipoles to deviate further from an antiparallel arrangement. Therefore we prepared the *S*(+)-2-(methoxymethyl)pyrrolidino derivative PMPDQ.²² As we anticipated, the SHG of this material showed great improvement over MBPDQ and was ~ 28 U. The crystals of PMPDQ, however, showed poor refinement in the structure analysis, perhaps owing to some free motion of the methoxymethyl group. The molecular structure could not be established fully even though the crystal space group and unit cell dimensions could be assigned ($P2_12_12_1$; $a = 15.717$ Å, $b = 12.100$ Å, $c = 9.867$ Å; $\alpha = \beta = \gamma = 90^\circ$; $z = 4$) and the crystal packing could be determined.

The logical extension to these investigations that we considered was the synthesis of the bis(*S*(+)-2-methoxymethylpyrrolidino) derivative, DMPDQ. It was hoped that the presence of two methoxymethyl groups would create enough steric hindrance between molecules to prevent free motion of these ether chains and help in the crystal structure refinement. It was also hoped that increasing the number of stereogenic centers in a rigid

(24) Kurtz, S. K.; Perry, T. T. *J. Appl. Phys.* **1968**, *39*, 3798.

(25) MOPAC93, Fujitsu Inc.

(26) Dewar, M. J. S.; Zoebisch, E. G.; Healy, E. F.; Stewart, J. J. P. *J. Am. Chem. Soc.* **1985**, *107*, 3902.

(27) (a) Dupuis, M.; Karna, S. *J. Comput. Chem.* **1991**, *12*, 487. (b) Kurtz, H. A.; Stewart, J. J. P.; Dieter, K. M. *J. Comput. Chem.* **1990**, *11*, 82.

Table 1. Crystallographic Data for DMPDQ

molecular formula	C ₂₂ H ₂₈ N ₄ O ₂
space group	<i>P2</i> ₁
<i>a</i> , Å	13.902(3)
<i>b</i> , Å	8.311(4)
<i>c</i> , Å	9.203(2)
β , deg	102.26(1)
<i>V</i> , Å ³	1039.1(7)
<i>z</i>	2
ρ_{calcd} , g cm ⁻³	1.22
$\mu(\text{Cu K}\alpha)$, cm ⁻¹	6.01
no. of unique reflns	2115
no. of reflns with $I \geq 2\sigma_I$	2059
<i>R</i>	0.034
<i>R</i> _w	0.054

framework would coax the molecular dipoles further away from an antiparallel arrangement, thus improving the quadratic nonlinear optical properties.

As described in the Experimental Section, crystals of DMPDQ were grown from acetonitrile solution, and the crystal structure analysis showed that the refinement went through smoothly in contrast to PMPDQ. The crystal belongs to the noncentric space group *P2*₁. The unit-cell parameters and relevant structure analysis data are collected in Table 1. The fractional atomic coordinates, important bond lengths, bond angles, and dihedrals in the molecule are presented in Table 2. The bond lengths indicate that the unsaturated ring has benzenoid character, an effect arising from the polarization of charge from the amino end to the cyano end and observed in all molecules of this class.^{21,22} The molecular structure (Figure 2a and Table 2) reveals also a strong twist of the diaminomethylene unit with respect to the benzenoid plane, again a feature common among these molecules. The relevance of this molecular twist to the hyperpolarizability is discussed in detail later.

The SHG capability of DMPDQ was determined using the Kurtz–Perry powder method²⁴ and gave the highest value, $\sim 55 \pm 10\%$ U, in this series of push–pull quinonoid systems, for powders with particle sizes in the range 50–200 μm . The saturation of the SHG intensity indicated that the material is phase-matchable. Examination of the crystal packing (Figure 2b) reveals that the molecular dipoles show strong deviation from an antiparallel alignment and are nearly perpendicular to each other. We have collected in Table 3 the intervector angle, α , between the near-neighbor molecular dipoles (as defined in the Introduction) in MBPDQ, PMPDQ, and DMPDQ. It may be noted that MBPDQ and DMPDQ have only two molecules in the unit cell and the intervector angle is unique. In PMPDQ, there are four molecules per unit cell and hence two inequivalent intervector angles. If we assume that the polar axis of the crystals is along the net dipole vector of the molecules in the unit cell, the angle between this unique axis and the molecular dipoles are 84° in MBPDQ, 27.5°, and 121.5° in PMPDQ and 51.5° in DMPDQ. It is noteworthy that the angle in DMPDQ is quite close to the optimal angle for efficient SHG.¹⁵ Table 3 shows that the calculated $\beta(0)$ values of the three molecules are nearly the same; however, the SHG capabilities show profound changes. A simple model of vector addition may be used to obtain a qualitative understanding of the influence of the angle, α on the bulk SHG capability. The sum of two vectors with magnitude β and having an intervector angle α , can easily be shown to be $f\beta$, where $f = \{2(1 + \cos \alpha)\}^{1/2}$. The enhancement

Table 2. (a) Fractional Atomic Coordinates of Non-H Atoms, (b) Significant Bond Lengths, and (c) Significant Bond Angles and Dihedral Angles in DMPDQ from Single-Crystal X-ray Analysis (Atom Labelings Shown in Figure 2)

(a)			
atom	<i>x</i>	<i>y</i>	<i>z</i>
C(1)	0.7488(1)	0.4000	1.1030(2)
C(2)	0.7324(1)	0.3404(3)	0.9576(2)
C(3)	0.7339(1)	0.4417(3)	0.8397(2)
C(4)	0.7494(1)	0.6082(3)	0.8602(2)
C(5)	0.7649(1)	0.6660(3)	1.0070(2)
C(6)	0.7659(1)	0.5647(3)	1.1257(2)
C(7)	0.7513(1)	0.2855(3)	1.2252(2)
C(8)	0.7490(1)	0.7139(3)	0.7359(2)
N(9)	0.8286(1)	0.2742(3)	1.3371(2)
C(10)	0.9295(1)	0.3310(4)	1.3313(2)
C(11)	0.9884(2)	0.2860(4)	1.4864(3)
C(12)	0.9143(2)	0.2838(4)	1.5830(3)
C(13)	0.8253(2)	0.2075(4)	1.4846(2)
C(14)	0.9659(2)	0.2540(4)	1.2048(3)
O(15)	0.9511(1)	0.0873(3)	1.2078(2)
C(16)	0.9767(2)	0.0088(7)	1.0865(3)
N(17)	0.6753(1)	0.1852(3)	1.2196(2)
C(18)	0.5720(1)	0.2283(4)	1.1519(2)
C(19)	0.5185(2)	0.0666(4)	1.1383(3)
C(20)	0.5984(2)	-0.0606(4)	1.1628(3)
C(21)	0.6818(1)	0.0181(3)	1.2729(2)
C(22)	0.5336(2)	0.3472(4)	1.2496(3)
O(23)	0.5436(1)	0.2781(4)	1.3900(2)
C(24)	0.5083(3)	0.3760(8)	1.4915(5)
C(25)	0.7404(2)	0.6558(4)	0.5911(2)
N(26)	0.7327(2)	0.6087(5)	0.4722(2)
C(27)	0.7584(2)	0.8799(4)	0.7540(2)
N(28)	0.7662(3)	1.0176(4)	0.7683(3)

(b)	
bond	bond length (Å)
C(1)–C(2)	1.399(2)
C(1)–C(6)	1.398(3)
C(1)–C(7)	1.468(2)
C(2)–C(3)	1.377(3)
C(3)–C(4)	1.407(3)
C(4)–C(5)	1.407(2)
C(4)–C(8)	1.441(3)
C(5)–C(6)	1.377(3)
C(7)–N(9)	1.324(2)
C(7)–N(17)	1.339(2)
C(8)–C(25)	1.399(2)
C(8)–C(27)	1.392(3)
C(25)–N(26)	1.146(3)
C(27)–N(28)	1.155(4)

(c)	
bond angle/dihedral	angle (deg)
C(1)–C(7)–N(9)	121.7(2)
C(1)–C(7)–N(17)	118.9(1)
C(7)–N(9)–C(10)	124.3(2)
C(7)–N(9)–C(13)	124.3(2)
C(7)–N(17)–C(18)	123.5(2)
C(7)–N(17)–C(21)	125.7(2)
N(9)–C(7)–N(17)	119.3(2)
C(10)–N(9)–C(13)	111.4(2)
C(18)–N(17)–C(21)	110.7(2)
C(1)–C(7)–N(9)–C(10)	20.4
C(1)–C(7)–N(17)–C(18)	33.4
C(2)–C(1)–C(7)–N(17)	53.8
C(3)–C(4)–C(8)–C(25)	4.7
C(5)–C(4)–C(8)–C(27)	3.7
C(6)–C(1)–C(7)–N(9)	54.2

or reduction factor, f , for the three materials are presented in Table 3; for PMPDQ, the two α 's are employed successively to evaluate f . The increased rigidity of the stereogenic center environment in PMPDQ compared to MBPDQ and the increase in the number of such stereogenic centers in DMPDQ lead to

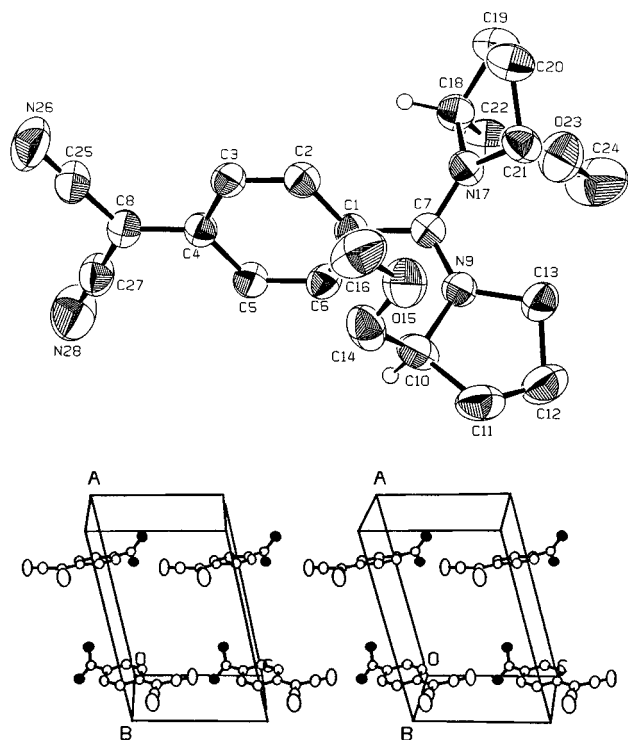


Figure 2. (a, top) Molecular structure of DMPDQ from single-crystal X-ray analysis; H atoms of only the stereogenic centers are shown. (b, bottom) Stereoview of the unit cell along the *b* axis; all atoms except N (shown as filled circle) of the (methoxymethyl)pyrrolidine groups are omitted for clarity.

Table 3. Static β Values, Interdipole Vector Angles α from Crystal Structure Analysis, the Computed Enhancement/Reduction Factor f (See Text for Details), and the Powder SHG Values for Three SHG-Active Compounds

molecule	$-\beta(0)$ (10^{-30} esu)	interdipole vector angle, α (deg)	enhancement or reduction factor, f	powder SHG (U)
MBPDQ ^a	51.0	168	0.21	3
PMPDQ ^a	51.4	94, 149	0.73	28
DMPDQ	50.2	103	1.25	55

^a Reference 22.

progressive deviation of dipole vectors from an antiparallel arrangement, reflected in the increase in the value of the factor f . Since the β values of the three compounds are nearly the same, the SHG intensities follow the trend of f , illustrating the crucial influence of the dipole alignment on the NLO characteristic of the bulk material.

In an effort to search for other features of the molecular packing that may be relevant to their NLO properties, we have examined the interatomic distances between molecules in the crystals of MBPDQ, PMPDQ, and DMPDQ. In DMPDQ there are short distances of 2.501 and 2.563 Å between aromatic ring H atoms and cyano group N atoms of neighboring molecules along the *b* and *c* axes leading to molecular sheets approximately parallel to the *bc* plane. Such intermolecular interactions are not observed in MBPDQ or PMPDQ. Significantly, in none of the three cases do we find such interactions between molecules which are oriented with the inter dipole vector angle, α , discussed above; in DMPDQ, these molecules form neighbors along the *a* axis. Therefore it appears that the C–H···N intermolecular interactions do not have any direct bearing on the SHG efficiencies of these materials, even though

they perhaps exert a strong stabilizing influence in the crystal packing in DMPDQ.

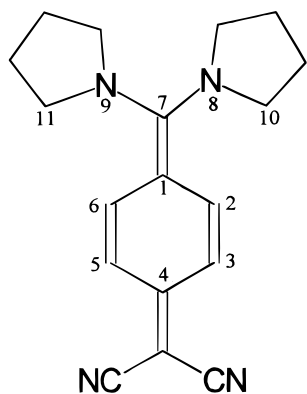
Though there are numerous reports of organic molecular materials with high solid-state SHG capability, there are only a dozen or so with completely characterized crystal structures, showing strong and stable solid-state SHG of the order of 100 U and having acceptable optical transparency. Several of these are handicapped by relatively low melting points of 100–150 °C.²⁸ In light of these facts, we believe that DMPDQ represents an interesting and significant advance in the field of molecular materials with strong solid-state SHG capability, optical transparency and thermal stability. The ease of synthesis and crystallization of this material and the amenability to further modifications are additional attractive features. The design and investigation of DMPDQ has also illustrated the effect of the placement of the stereogenic center on the alignment of molecular dipoles in crystals which can be used as a guideline for obtaining improved SHG in molecular materials.

In the family of diamino-substituted dicyanoquinodimethanes, so far we have investigated the molecular and crystal structure of seven compounds, including DMPDQ discussed above. A common feature among the molecular structures of these compounds is the strong twist of the diaminomethylene unit with respect to the quinonoid plane. We refer to this angle as θ and its values are collected in Table 4. Table 4 also presents the value of θ obtained by full AM1 optimization of the geometry. It is immediately obvious that the $\theta(\text{CS})$ and $\theta(\text{AM1})$ show poor agreement in the case of the three molecules involving saturated six-membered ring heterocycles for the amino moiety. This may be attributed to the fact that the bulkier and conformationally more flexible six-member rings have quite different steric interactions in the gas phase (simulated by the calculations) and the crystalline phase. In the case of the other four molecules the agreement of the two θ values is much better. Table 4 also contains the β values calculated for the two geometries. The $\beta(\text{AM1})$ are found to be smaller than the $\beta(\text{CS})$ in all cases. The smaller value of $\beta(\text{AM1})$ relative to $\beta(\text{CS})$ throughout the series arises mainly due to the difference in the bond lengths in the quinonoid framework in the CS and AM1 geometries. An insight into this may be gained by quantifying the quinonoid–benzenoid character of these geometries, using the parameter QBC defined by us earlier.²⁰ The CS geometries are more benzenoid than the AM1 geometries, since the former are the optimal geometries of those molecules in a strongly polar crystal environment; hence the CS geometries have larger QBC values than the AM1 geometries. We have shown²⁰ using model calculations on 7,7-diamino-8,8-dicyanoquinodimethane, that the β values decrease monotonically with the QBC values, when the β calculations are carried out without the presence of a simulated external field. The β values reported in Table 4 are calculated in the same fashion, hence the lower β for the AM1 structures having smaller QBC values.

The interesting aspect that emerges from a careful analysis of the θ and β values discussed above is the correlation between $\theta(\text{AM1})/\theta(\text{CS})$ and $\beta(\text{AM1})/\beta(\text{CS})$ also presented in Table 4. A minor variation of θ from

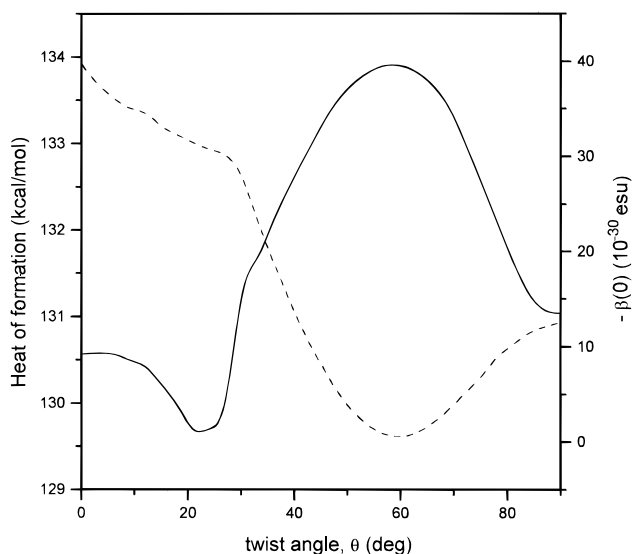
Table 4. Twisting Angles θ from Crystal Structure (CS) and Optimized AM1 Geometries, Corresponding Static β Values, the Ratio of Twisting Angles ($\theta_{\text{AM1}}/\theta_{\text{CS}}$), and the Ratio of β Values ($\beta_{\text{AM1}}/\beta_{\text{CS}}$) for the Seven Diamino-Substituted Dicyanoquinodimethanes Whose Crystal Structures Have Been Investigated

molecule	twisting angle (deg)		$-\beta(0)$ (10^{-30} esu)		$\theta_{\text{AM1}}/\theta_{\text{CS}}$	$\beta_{\text{AM1}}/\beta_{\text{CS}}$	ref
	CS	AM1	CS	AM1			
DMDQ	48.6	34.0	54.3	11.9	0.700	0.219	21
DPIDQ	46.8	38.6	54.9	19.8	0.825	0.361	21
DPZDQ	43.0	38.9	53.9	16.6	0.905	0.308	21
MBPDQ	49.9	45.5	51.0	27.6	0.912	0.541	22
DMPDQ	54.0	50.8	50.2	35.8	0.937	0.713	this work
PMPDQ	58.2	57.9	51.4	38.7	0.995	0.753	22
DPDQ	56.7	59.3	52.6	39.5	1.045	0.751	29

**Figure 3.** Molecular structure of DPDQ with relevant atom labeling.

AM1 to CS geometry is associated with a small variation of β between these geometries and a larger variation of θ is associated with a relatively larger change in β . This trend is followed through the series except for a minor discrepancy. This suggested to us that within a molecule, the hyperpolarizability would have a strong dependence on the molecular twist angle, θ . We discuss below the analysis of this problem using semiempirical calculations on the model compound DPDQ; the molecular framework indicating the relevant atom labelings is shown in Figure 3. We note that DPDQ shows interesting solvent-dependent polymorphism; the crystals obtained from acetonitrile are SHG inactive and the crystals from chloroform show a novel kind of solvate-switchable SHG.²⁹ However, in the following discussion we are interested only in the molecular structure of DPDQ which is nearly identical in both the crystals.

The AM1 optimized geometry of DPDQ is very close to the one obtained from the crystal structure analysis, especially with regard to the twist angle (Table 4). Starting from the crystal structure geometry having nearly C_2 point group symmetry, the twist angle, θ (dihedral angle 8–7–1–2 or 9–7–1–6; see Figure 3) was varied in 3° intervals to 0° on one side and 90° on the other and geometry optimization carried out at each point imposing a C_2 symmetry constraint. The point closest to the crystal structure geometry has $\theta = 57^\circ$. We note that each θ point optimization was carried out using the optimized geometry at the previous point as the starting structure to ensure smooth geometry changes. The imposition of C_2 symmetry does not cause any marked changes in the heat of formation of the optimized structures; it helps to make the geometry changes more controlled and smooth and suppresses unrealistic spikes that otherwise arise in the curve

**Figure 4.** Plot of the heat of formation, ΔH_f (---) and the static hyperpolarizability, $-\beta(0)$ (—) versus twist angle, θ for DPDQ (see text for the definition of θ).**Table 5.** Heat of Formation (ΔH_f) and Static Hyperpolarizability ($\beta(0)$) at Various Twist Angles (θ) for DPDQ along with the Square of the Transition Moment (μ^2), Dipole Moment Change ($\Delta\mu$), and Energy Difference (ΔE) between the Ground and First Excited State

θ (deg)	ΔH_f (kcal/mol)	$-\beta(0)$ (10^{-30} esu)	μ^2 (esu ²)	$-\Delta\mu$ (D)	ΔE (eV)
0	133.9	9.3	0.8770	0.63	2.992
9	133.4	8.6	1.5688	0.50	2.811
18	133.1	3.8	1.8093	0.52	2.600
27	132.9	4.5	2.0034	1.16	2.393
36	131.6	23.3	2.1715	3.47	2.170
45	130.5	33.2	2.0828	5.32	2.150
54	129.7	38.9	1.7806	7.45	2.146
57	129.6	39.6	1.6333	8.14	2.151
63	129.7	38.9	1.2873	9.46	2.163
72	130.1	31.5	0.6816	11.51	2.206
81	130.9	18.9	0.1644	13.59	2.259
90	130.9	13.5	0.0007	15.45	2.269

owing to the conformational flexibility associated with the pyrrolidine ring. Table 5 presents the calculated heats of formation and the β at 9° intervals, and the variation of ΔH_f and β with the angle θ is plotted in Figure 4 using all the data points calculated above. From $\theta = 60^\circ$, a value close to that found in the crystal structure geometry ($\sim 57^\circ$), the heat of formation rises by about 1.3 kcal/mol at 90° twist and by nearly 4.3 kcal/mol at the planar geometry. There is a small discontinuity at about 27° . Inspection of the optimized geometries reveals that when $\theta = 0^\circ$, the dihedral angle, 10–8–7–1 (τ) is $\sim 80^\circ$ ie., the pyrrolidine rings are nearly perpendicular to the plane of the diaminomethylene moiety whereas when $\theta = 90^\circ$, $\tau \sim 0^\circ$. The slow

(29) Ravi, M.; Narayana Rao, D.; Cohen, S.; Agranat, I.; Radhakrishnan, T. P. *J. Mater. Chem.* **1996**, *6*, 1853.

rotation of the pyrrolidine ring with respect to the diaminomethylene unit when θ varies from 0° to 90° , takes a sudden jump at $\theta = 27^\circ$, and this appears to be the cause of the discrepancy in the monotonous fall of ΔH_f noticed at this point. The value of β is also found to go through a small anomaly as a consequence of this; initially it decreases slightly from the planar geometry and then rises smoothly until $\theta = 57^\circ$, followed by a decline to the perpendicular geometry. The most significant observation here is that the β value goes through a maximum close to the θ corresponding to the optimized geometry of the molecule. This is rather unusual and in contrast to the behavior observed in other systems investigated previously,^{30,31} where β was found to decrease monotonously with increasing molecular twist. We analyze below the factors that lead to this interesting effect.

The simple two-state model of Oudar²³ is based on a description of β in terms of the ground state and a single excited state of the molecule and shows that the static hyperpolarizability, $\beta(0)$ depends on the square of the transition dipole moment, μ^2 (directly proportional to the oscillator strength) and energy of this excitation, ΔE , as well as the change in dipole moment, $\Delta\mu$ between the ground and the excited state:

$$\beta(0) \propto \{\mu^2 \Delta\mu / (\Delta E)^2\}$$

Our earlier studies²⁰ on the model system 7,7-diamino-8,8-dicyanoquinodimethane have shown that the two-state picture fails to predict quantitatively the hyperpolarizabilities of this class of molecules; however, the qualitative trends are reproduced well. Therefore we have estimated, using semiempirical AM1/CI computations, the values of μ^2 , $\Delta\mu$, and ΔE in DPDQ at various twist angles using the geometries optimized above (Table 5 presents the data at 9° intervals). The variation of $-\beta(0)$, μ^2 , $-\Delta\mu$, and ΔE with θ for the full data set is depicted in Figure 5 (note that the absolute values of the y -axis variables are not indicated in the figure to make the comparison of trends easier; however, the relative values are to scale). It is seen that the μ^2 rises initially up to $\theta \sim 40^\circ$ and then decreases continuously to 90° . The $-\Delta\mu$ shows a small decline from 0° to 15° followed by a gradual rise to 30° and a stronger and nearly linear increase subsequently. This arises from the strong increase in the ground-state dipole moment and a small decrease of the excited-state dipole moment on going from the planar ($\mu_g = 11.46$ D, $\mu_e = 10.83$ D) to the orthogonal ($\mu_g = 21.58$ D, $\mu_e = 6.13$ D) geometry. It is noteworthy that the change in dipole moment on excitation is very large even at the optimized geometry, and we believe that this is one of the important factors that contributes to the large β of this class of molecules. The ΔE decreases continually from 0° to about 50° and then registers a gradual increase to 90° . Leaving aside the anomalous behavior of the various quantities in the range 15 – 30° which arises from the rotation of the pyrrolidine ring as discussed earlier and is irrelevant to the main focus of our analysis here, the trends of the three quantities noted above influence the β as follows.

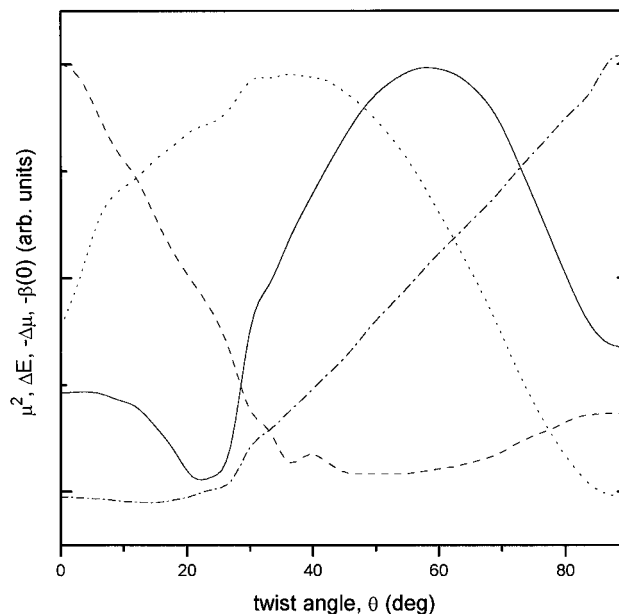


Figure 5. Plot of the square of the transition moment, μ^2 (\cdots), energy difference, ΔE ($---$) and the dipole moment change, $-\Delta\mu$ ($- \cdot -$) between the ground and excited state and the static hyperpolarizability, $-\beta(0)$ ($-$) versus the twist angle, θ for DPDQ (see text for definition of θ).

The maximum in μ^2 and the minimum in ΔE are expected to lead to a maximum in β at some value of θ between 40° and 50° . The strong rise of $\Delta\mu$, however, shifts this maximum to an angle closer to 60° . Thus we find that the hyperpolarizability goes through a maximum at a twist angle close to that found in the optimal structure. The transition moment appears to be the dominant factor contributing to this. We have repeated these studies with other members of the family of diamino-substituted dicyanoquinodimethanes and found similar trends showing that this is a general effect in this class of molecules.

Conclusion

We have presented in this paper the details of synthesis, characterization, and crystal structure of a new member of the class of push-pull quinonoid molecular materials that we have developed in recent years. DMPDQ is found to have the highest powder second harmonic generation capability (~ 55 U) in the series, and this is in good accord with the progression of interdipole vector angles toward an orthogonal orientation in this family of crystals. The improvement in the alignment of dipoles was achieved by controlling the placement of the stereogenic centers in these compounds. The ease of synthesis and crystallization, near transparency through the visible window, good thermal stability up to $\sim 250^\circ\text{C}$, and strong phase-matchable second harmonic generation are the positive features of the new molecular material which should make it a significant entry into the class of crystalline molecular materials with potential quadratic NLO applications. Though a variety of materials based on thin films, polymers, etc., showing strong NLO characteristics have been reported, we believe that crystalline materials will continue to play an important role in the development of advanced materials and molecular devices because of the advantage they offer in terms of a direct insight into the structural aspects that is vital

(30) Lequan, M.; Lequan, R. M.; Chane-Ching, K.; Barzoukas, M.; Fort, A.; Bravic, G.; Chasseau, D.; Barrans, Y.; Huche, M. *Chem. Phys. Lett.* **1993**, *213*, 71.

(31) Lequan, M.; Lequan, R. M.; Chane-Ching, K.; Bassoul, P.; Bravic, G.; Barrans, Y.; Chasseau, D. *J. Mater. Chem.* **1996**, *6*, 5.

for fine-tuning and improving the physical properties. The present study illustrates this point.

We have also analyzed in detail the close correlation between the strong molecular twist observed in the series of diamino-substituted dicyanoquinodimethanes and their hyperpolarizabilities. The significant result from the semiempirical computational study is that the β as a function of the twist, θ , goes through a maximum at the angle corresponding to the optimal geometry. The factors that contribute to this are analyzed in terms of the two-state model. The fact that these molecules manifest their highest possible values of β at the θ observed in their crystals is very encouraging for our continuing efforts in the development of these molecular materials.

Acknowledgment. T.P.R. and D.N.R. thank the Department of Science and Technology, New Delhi, for financial support and M.R. thanks the Council of Scientific and Industrial Research, New Delhi for the senior research fellowship. We thank also Mr. Kiran for help with some of the computations.

Supporting Information Available: Listing of bond distances, angles, least-squares planes, and structure factors for DMPDQ and a table providing the full data plotted in Figures 4 and 5 (12 pages); details of crystal structure analysis (15 pages). Ordering information is given on any current masthead page.

CM960530N